Ordered Carbonaceous Frameworks: A new class of carbon materials with molecular-level design

Journal:	*ChemComm*
Manuscript ID	CC-FEA-12-2021-007228.R1
Article Type:	Feature Article

SCHOLARONE™
Manuscripts

Please do not adjust margins

ARTICLE

Ordered carbonaceous frameworks: A new class of carbon materials with molecular-level design

Takeharu Yoshii,*[a] Koki Chida,[a] Hirotomo Nishihara,*[ab] and Fumito Tani*[c]

Ordered carbonaceous frameworks (OCFs) are a new class of carbon materials with a three-dimensional ordered structure synthesized by simple carbonization of metalloporphyrin crystals with polymerizable moieties. Carbonization via solid-state polymerization results in the formation of graphene-based ordered frameworks in which regularly aligned single-atomic metals are embedded. These unique structural features afford molecular-level designability like organic-based frameworks together with high electrical conductivity, thermal/chemical stability, and mechanical flexibility, towards a variety of applications including electrocatalysis and force-driven phase transition. This feature article summarizes the synthetic strategies and characteristics of OCFs in comparison with conventional organic-based frameworks and porous carbons, to discuss the potential applications and further development of the OCF family.

1. Introduction

Carbon materials have become indispensable in our life, since they are used in a wide variety of applications such as electrode materials, adsorbents, catalytic supports, environmental purification, airplanes, automobiles, medicines, etc.[1, 2] In research and industrial applications, typical advantages of carbons are right weight, high thermal/electrical conductivity, chemical/thermal durability, and mechanical strength/flexibility. In addition, as typified by activated carbons, micro- and mesopores can be developed in carbon materials, affording high specific surface areas up to 2000-4000 m^2 g^{-1}.[3] However, these nanoporous carbon materials are generally composed of disordered stacking and aggregation of defective graphene sheets, and it is difficult to exactly describe the chemical structures, resulting in a major obstacle in the study and further development of nanoporous carbons. In most cases, nanoporous carbon materials have been synthesized by processes that rely on empirical parameters, and thus, the preparation with well-designed structures at the molecular level has been still a challenging target. Crystalline microporous materials, such as zeolites, metal organic frameworks (MOFs), and covalent organic frameworks (COFs), are counterpart of disordered nanoporous carbon materials and have well-defined chemical structures with uniform-sized ordered micropores at an Å level.[4-6] A wide variety of frameworks can be obtained by changing precursors and synthesis protocols.

To achieve such ordered and uniform structures in nanoporous carbon materials, a hard template method has been adopted.[7] In that method, carbon is loaded into an inorganic template under an inert gas atmosphere, followed by a removal of the template by a chemical etching process. The resulting carbon is obtained as a negative replica of the original template. If a crystalline template is used, the structure regularity can be reflected in the templated carbon. At an early stage, silica gel was used as a hard template to obtain amorphous porous carbons in 1982,[8] and since then, a wide variety of three dimensional (3D) ordered porous carbons have been synthesized using oxide templates such as zeolite,[9-15] mesoporous silicas,[16, 17] and silica opals.[18, 19] The resulting materials with structure ordering are known as ordered porous carbons including "ordered microporous carbons", "ordered mesoporous carbons", and "ordered macroporous carbons". More recently, the hard-template method has been expanded to the synthesis of graphene-based 3D nanoporous materials using Ni-foam,[20] Al_2O_3 and MgO nanoparticles.[21-24] In contrast to the hard template method, a soft template method has been developed since around 2000s, and ordered mesoporous carbons were fabricated from block copolymers,[25] and from the mixture of thermosetting polymer and surfactant micelles.[26, 27] The history of the template techniques was summarized in some review papers,[13, 28] and we avoid overlapping of contents in this article. Despite the structural controllability of the template technique, it has been challenging to regularly embed single-atomic metal species like MOFs.

[a.] Institute of Multidisciplinary Research for Advanced Materials, Tohoku University, 2-1-1 Katahira, Aoba-ku, Sendai, Miyagi, 980-8577, Japan.
[b.] Advanced Institute for Materials Research, Tohoku University, 2-1-1 Katahira, Aoba-ku, Sendai, Miyagi, 980-8577, Japan.
[c.] Institute for Materials Chemistry and Engineering, Kyushu University, 744 Motooka, Nishi-ku, Fukuoka 819-0395, Japan.
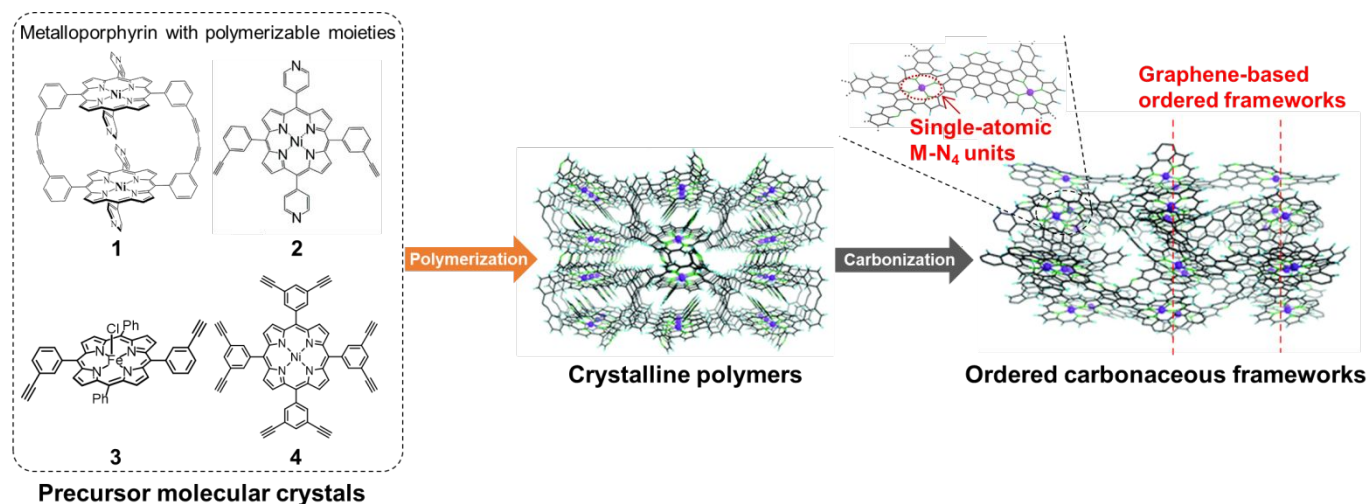Email: takeharu.yoshii.b3@tohoku.ac.jp, hirotomo.nishihara.b1@tohoku.ac.jp, tanif@ms.ifoc.kyushu-u.ac.jp

Fig. 1 Synthetic scheme of ordered carbonaceous frameworks (OCFs) by the simple carbonization of metalloporphyrins (**1**-**4**).

As another strategy, the direct conversion of crystalline organic-based frameworks into microporous carbons has emerged. In the past decade, pyrolysis of organic-based frameworks, such as MOFs and COFs, has been especially widely attempted.[29-32] Although microporous carbons had been obtained by such a method, the original crystalline structures cannot be maintained at high temperature, resulting in the formation of disordered carbonaceous materials in most cases. Carbon materials with ordered frameworks together with regularly aligned metals, which can be considered as "MOF-like carbons", are ideal materials not only for basic research but also for applications such as electrocatalysis. In that regard, the authors have recently developed exceptional carbon materials with well-defined ordered structures, called ordered carbonaceous frameworks (OCFs).[33-36] A simple carbonization of metalloporphyrin crystals with polymerizable moieties (**1**-**4**) yields three-dimensional graphene frameworks reflecting the original ordered structures (Fig. 1). Furthermore, single-atomic metal species are immobilized in OCFs with a regular arrangement, and this is the most important structural difference between traditional "ordered porous carbons" and OCFs.

Due to the above-mentioned unique features, the advantages of both MOFs and carbon materials are simultaneously realized in OCFs. The properties of OCFs are compared with MOFs and porous carbon materials in Fig. 2. OCFs possess a molecular-level ordered structure, similar to MOFs. On the other hand, OCFs are composed of non-stacked graphene sheets and have features not found in MOFs, such as electrical conductivity and chemical/thermal stability, which are advantages unique to carbon materials. Although MOFs and COFs are also used to electrochemical applications, they need to be mixed with a large amount of conductive additives because of their very high electric resistivity. OCFs have more than 10^{10} times higher electric conductivity compared to their organometallic precursors and are free from the restrictions caused by poor electric conductivity.[33] Moreover, OCFs contains a significant amount of metal as a form of single-atomic species. Therefore, OCFs have the potential to be used

in a variety of application, e.g., supercapacitors, electrocatalysis and gas separation/storage.

The purpose of this feature article is to give a brief introduction to OCFs. The synthesis of OCFs is based on the direct carbonization of crystalline organometallic solids which are appropriately designed to retain the molecular-level structure. The synthesis process is much different from the traditional template techniques, which were summarized in other review papers.[13, 28] To distinguish the synthetic strategy as well as the resulting structures from other porous carbon materials synthesized by direct carbonization of organic-based frameworks, we first summarise the history of the direct carbonization especially focusing on the structure preservation during carbonization in chapter 2. Then, the synthetic strategy of OCFs is described together with the structures and characteristics of the resulting OCFs in chapter 3. Finally, applications and future potentials of OCFs are discussed.

	OCFs	MOFs	Microporous carbons e.g., activated carbon
Components	Graphene frameworks with single-atomic metals	Organic ligands and metal ions or clusters	Disordered stacks of graphene sheets
Ordered structure	Yes	Yes	No
Electrical conductivity	High	Low	High
Chemical/thermal stability	High	Low	High
Metal content	9 wt% (OCF from **1**)	44 wt% (MOF-5)	No
Specific surface area	670 m²/g (OCF from **4**)	4500 m²/g (MOF-177)	2700 m²/g (MSC30)

Fig. 2 Properties of OCFs in comparison with MOFs and conventional microporous carbons.

2. Conventional synthesis of porous carbons from organic-based frameworks

2.1 Carbonization of organic-based frameworks

MOFs are characterized by well-defined 3D structures in **which metal ions or clusters are coordinated to organic ligands.[6] Because of highly developed and** uniformly sized micropores **as well as their diverse structures, MOFs are attracting attention for their use as a soft template for 3D nanoporous carbon materials. In the early stage, MOFs were used as templates for carbon synthesis via polymer formation inside the micropores. Xu *et al*. pioneered in 2008 the synthesis of micro**porous carbons with a specific surface area (S_{BET}) of 2872 m^2 g^{-1} by carbonization polyfurfuryl alcohol formed within the pores of MOF-5.[29] In subsequent studies, the similar protocol was employed for zeolitic imidazolate framework-8 (ZIF-8) and Al-based porous coordination polymer (Al-PCP) to prepare nanoporous carbons.[37-40] Later on, Kitao *et al*. have extended the concept of the MOF-templating method to obtain graphene nanoribbons (Fig. 3a).[41] Upon introduction of perylene into MOFs, the perylene aligned along one-dimensional nanochannels. The thermal polymerization of these aligned perylene enabled the formation of armchair-type graphene nanoribbons with atomic-level accuracy at the bulk scale.

The development of direct conversion approach was an important breakthrough in MOF-based carbon synthesis.[31, 32] Since MOFs contain organic ligands as their constituents, carbon materials can be obtained by direct pyrolysis of MOFs and removal of inorganic components without infiltration of carbon sources. In 2010, Hu *et al*. prepared nanoporous carbons by the direct pyrolysis of MOF-5 for the first time.[42] In this case, the Zn clusters in MOF-5 were vaporized during the heat treatment, yielding a porous carbon without inorganic impurities (S_{BET}: 1812 m^2 g^{-1}). Yamauchi *et al*. studied the direct carbonization approach in more detail using Al-PCP as a precursor.[30] By pyrolysis of Al-PCP at 1023 K, followed by HF treatment, nanoporous carbons were obtained with an extremely high S_{BET} of 5500 m^{2}g^{-1} and a large pore volume of 4.3 cm^{3}g^{-1}. They continued to report the synthesis including nanoporous carbons from commercially available ZIF-8, and carbon nitride fibres from Al-PCP with a nitrogen source of dicyandiamide.[32, 43-45] At about the same time, Park *et al*. applied such a method to a series of isoreticular MOFs to yield carbons with specific surface areas ranging from 1678 to 3174 m^{2}g^{-1}.[46, 47] Such early studies focused on synthesizing carbons with high specific surface area for supercapacitors and hydrogen uptake applications.[44, 48] These initial studies were followed by an avalanche of research on the synthesis of various types of MOF- and COF-derived carbon materials, including metal- or metal oxide-carbon composites,[49-51] N-, P-, or S-doped carbons,[52-56] and core-shell and hollow structural carbons.[57-60] In particular, a synthesis of core-shell type carbon composites from core-shell ZIF-8@ZIF-67 MOFs by Yamauchi *et al*. provided much insight for subsequent studies (Fig. 3b).[60] The significantly high capacitance has been achieved by the well-designed carbon composite, where the Zn-containing ZIF-8 in the core was converted to an N-doped carbon with high specific surface area, and the Co-containing ZIF-67 shell produced a highly graphitic carbon. Other noteworthy work

includes the synthesis of hollow particle-based nitrogen-doped carbon nanofibers by Lou *et al*.[61, 62] They developed one-dimensional hollow carbon composites suitable for supercapacitors by applying a combination of electrospinning and carbonization methods to fine ZIF-8 nanoparticles. Based on these innovative strategies, multiple types of MOF-based nano-architected carbon materials have been fabricated, exhibiting promising applications in various fields, including energy storage, catalysts, environmental remediation, and phototherapy. The progress of MOF-derived carbons for respective applications has been summarized in other review papers, e.g., supercapacitors,[63, 64] energy storage,[65-67] and catalysis.[68-71] However, the crystalline structures of MOFs easily collapsed during the carbonization process, and it had been a challenging target to prepare carbon materials in which the well-defined structures of organic-based frameworks are inherited.
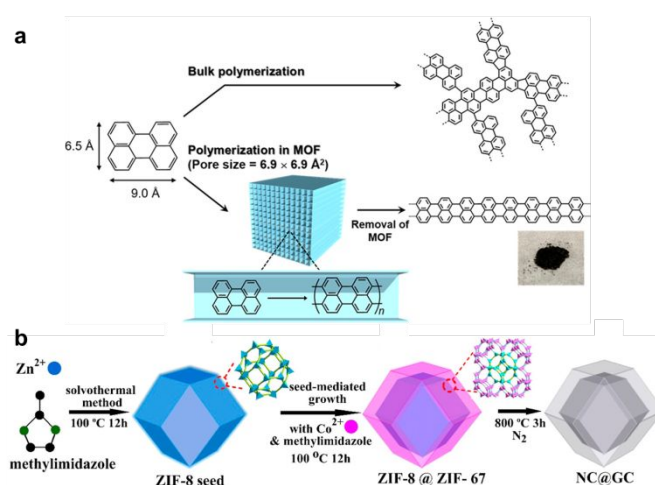

Fig. 3 (a) **Synthetic scheme of** armchair-type graphene nanoribbons using MOFs as a template. Reprinted with permission.[41] Copyright 2020 American Chemical Society. **(b) Synthetic scheme of** core-shell type carbon composites by the direct conversion of core-shell ZIF-8@ZIF-67 MOFs. Reprinted with permission.[60] Copyright 2015 American Chemical Society.

2.2 Structure-preserving carbonization of organic-based frameworks

In recent years, various strategic approaches have been proposed to obtain carbon materials that reflect the structures and morphology of precursors, which are summarized in the following subsections.

2.2.1 Morphology-preserving carbonization

The morphology preservation in MOF carbonization was first demonstrated in furfuryl alcohol-infiltrated fibre-shaped Al-PCP by Yamauchi *et al*. in 2011.[38] Afterwards, many studies have reported morphology-maintaining carbonization of organic-based frameworks.[57] Xu *et al*. reported the synthesis of one-dimensional (1D) carbon nanorods by self-sacrificial and morphology-preserving pyrolysis of a rod-shaped MOF-74 which was

synthesized using salicylic acid as a structural modulator (Fig. 4a).[72] More interestingly, the prepared carbon nanorods can be further converted to graphene nanoribbons with two to six-layer thickness through exfoliation process. 1D carbon nanorods were also fabricated by the direct conversion of fullerene (C_{60}) single-crystal nanorods and nanotubes at 2273 K by Ariga et al.[73] The above-mentioned works have reported the retention of exterior morphology of crystal at the micro-meter level, but the molecular-level structures of precursors were totally changed into amorphous carbon or graphene sheet structures. On the other hand, Ogoshi et al. demonstrated the retention of not only external crystal shape but also nanopores of a ring molecule in the carbonization of fibrous crystals composed of pillar[6]arene (Fig. 4b).[74] Interestingly, the micropore size of the obtained carbon was 4.10 Å, which was identical to that of the pillar[6]arenes assembly (4.09 Å). However, the crystalline structure of the precursor was lost, and the resulting porous carbon was intrinsically amorphous. Thus, the retention of ordered structures of precursors remained as a challenging target.
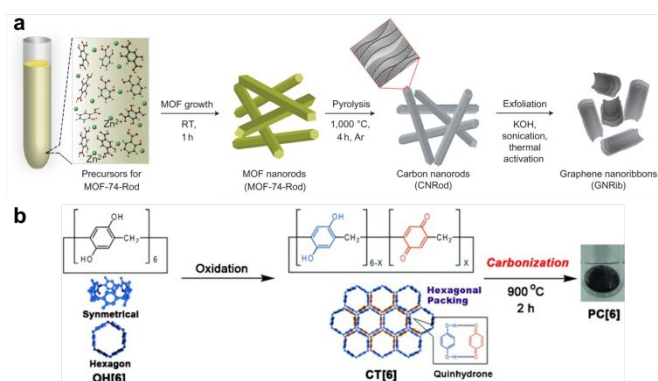

Fig. 4 (a) Synthetic scheme of one-dimensional carbon nanorods by morphology-preserving pyrolysis of a rod-shaped MOF-74, and graphene nanoribbons by further exfoliation. Reprinted with permission.[72] Copyright 2016 Springer Nature. (b) Synthetic scheme of carbon fibres preserving pore size and morphology of the pillar[6]arene assembly induced by 2D supramolecular polymerization. Reprinted with permission.[74] Copyright 2015 John Wiley and Sons.

2.2.2 Carbonization with preserving local structure around metals

One of the important current issues in catalysis field is the development of non-precious metal-based catalysts for oxygen reduction reaction (ORR) in fuel cells as an alternative to the expensive and rare platinum-based catalysts.[75] Carbon materials doped with heteroatoms (N, S, B, P, etc.) and transition metal species (Fe, Co, Ni, etc.) have been developed over the past few decades in pursuit of high activity and durability.[76-81] Conventionally, such catalysts have been prepared by pyrolysis of iron or cobalt precursors and nitrogen sources often together with carbon blacks, in which the single-atomic metals coordinated to nitrogen (Fe- or Co-N_x) species, so-called M-N-C units, serve as an active site for ORR.[82-89] Recently, pyrolysis of MOFs has emerged as

an promising strategy. Zeolitic imidazolate frameworks (ZIFs) are composed of tetrahedrally coordinated units of imidazolate linkers to single-atomic transition metals, such as Fe, Co, Cu, Zn.[90] Since the early-stage report on the formation of Co-N-C units from Co-type ZIFs by Liu et al. in 2011,[91, 92] carbonization of MOFs with preserving their local structure has been extensively studied, especially for electrocatalytic applications.[68, 93-95] In general, the heat treatment above 1023 K forms ORR active M-N-C structures from tetrahedral metal coordination, but at the same time, metal ions aggregate to form inactive nanoparticles.[50, 51] In other words, most metal species in the produced materials are not involved in ORR, even though high metal content is an advantage of MOF precursors. Thus, a key issue is how to control the local structure of the metal species with maintaining atomic-level metal dispersion during the carbonization process. Li et al. proposed a strategic approach that takes advantage of two MOFs (ZIF-8 and ZIF-67) having the same crystal structure with different metal species: Zn and Co, respectively (Fig. 5a).[96] Thus, a series of bimetallic ZIFs with various Zn/Co ratios can be synthesized between ZIF-8 and ZIF-67. In bimetallic ZIFs, the distance between Co atoms is increased by the insertion of Zn. Moreover, Zn can be evaporated above 1180 K, consequently preventing the formation of Co-Co bonds to form Co nanoparticles. The produced carbon contained as much as 4 wt% of atomic Co species without aggregation, which functioned as a high-performance ORR catalyst. Very recently, a new strategy utilizing the metal substitution ability of ZIF-derived carbons was proposed by Jia et al.[97] The Fe-N-C catalyst for ORR was synthesized by first preparing carbons possessing Zn-N_4 units from ZIF-8 and then reacting Zn with Fe by gaseous $FeCl_3$ to achieve a high active site density (1.92×10^{20} sites/g) with 100% site utilization efficiency (Fig. 5b).
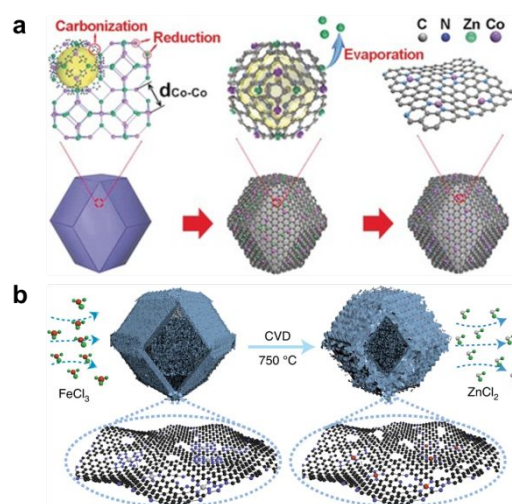

Fig. 5 (a) Synthetic scheme of single-atomic Co embedded in nitrogen-doped porous carbons by the direct carbonization of Zn/Co bimetallic ZIFs. Reprinted with permission.[96] Copyright 2016 John Wiley and Sons. (b) Synthetic scheme of Fe-N-C catalysts with a high active site density synthesized by

replacing Zn with Fe in a Zn-N-C carbon derived from ZIF-8. Reprinted with permission.[97] Copyright 2021 Springer Nature.

As described above, new approaches for the design and synthesis of carbon materials with controlled-local structure from MOFs are being developed one after another.[98-102] However, it had been challenging target to achieve the preservation of molecular-level ordered structures and single-metal structure at the same time. Also, increasing the amount of single-atomic metal sites embedded in carbonaceous frameworks needed to be further improved. As we will describe in the next chapter, OCFs are a new class of materials which can overcome the remaining challenges.

3. Synthesis and characterization of Ordered Carbonaceous Frameworks (OCFs)

3.1 Carbonization with preserving both ordered structure and local structure around metals

One of the most important features of organic porous frameworks is their ordered crystal structures. In the last decade, multiple types of carbon materials with highly developed nanopores have been synthesized from MOFs and COFs as summarized above, but most of them lose the original regularity. **Thus**, it has been still challenging to produce carbon materials while maintaining the molecular-level ordered structure of precursors. **An interesting attempt is to introduce an inorganic component into the MOF nanopores before carbonization, as reported by Lu _et al._ in 2011.[103] Prior to the carbonization, aminosilane was coordinated to the unsaturated chromium sites on the inner and outer surfaces of Cr-MIL-101 to strengthen the MOF framework during the heat treatment. XRD and STEM measurements confirmed the partially ordered structure in the final microporous inorganic hybrid material. This was the first example of a partial replication of the regularity of MOFs to the final composite, which was followed by an attempt to infiltrate of Ti(O-iPr)$_4$ into MOFs to form microporous titania.[104] Although these initial studies offered insights into the importance of strengthening the framework, it was still very challenging to directly reproduce the ordered structure of organic crystals in carbons without introducing inorganic additives.**

In contrast to the case of carbon synthesis, a large number of structure-maintaining polymerizations, called topochemical polymerization, have been reported.[105-107] When aligned monomers in the crystalline state are polymerized by external stimuli such as light, the resulting polymers can retain the ordered arrangement of monomers. Since the synthesis of polydiacetylene was first reported by Wegner in 1969, it has been extensively studied and applied in various fields including the organic film preparation.[108-112] These studies have inspired us a strategy for structure-preserving carbon synthesis via topochemical polymerization. The synthetic strategy is to first strengthen the crystal

framework structure by solid-state polymerization of precursor molecules, and then, the polymer is carbonized while replicating the original ordered structure.

In 2017, the authors revealed for the first time that a cyclic Ni porphyrin dimer (**1**, Ni$_2$-CPD$_{py}$)[113] is an exceptional precursor that can yield regularity-preserved carbon materials, called ordered carbonaceous frameworks (OCFs), by a simple heat treatment in an inert gas (see Fig. 1).[33] Thermal solid-state polymerization of diacetylene moieties in the molecular precursor crystal formed a crystalline polymer, which was further carbonized to the OCF without collapsing into an amorphous structure even at 1073 K. Owing to the thermal stability of Ni porphyrin units, regularly aligned single-atomic Ni species were immobilized in the produced carbons with Ni-N$_4$ coordination, which can catalysed the electrochemical CO$_2$ conversion into CO with high Faraday efficiency. The first OCF synthesis from Ni$_2$-CPD$_{py}$ was followed by the expansion of the precursor molecules. A new type of OCF was prepared from Ni-porphyrin monomer with polymerizable ethynyl groups (**2**), which can be synthesized much more readily than the cyclic dimer molecule of Ni$_2$-CPD$_{py}$ (**1**).[34] The authors subsequently demonstrated that Fe porphyrin with two ethynyl groups (**3**) also produce OCFs.[35] Very recently, OCFs with developed microporosity (S_{BET}: 673 m^2/g) was successfully synthesized by designing a precursor of Ni porphyrin monomer with eight ethynyl moieties (**4**).[36] The porous OCFs exhibited unique mechanical flexibility due to the non-stacked graphene frameworks, demonstrating a force-responsive phase transition. As mentioned above, the authors are creating a new class of carbon materials of OCFs by carbonizing organic crystals while keeping the original ordered structure. Such materials possess molecular-level designability like MOFs as well as the advantages of stability and conductivity as carbon materials, and therefore, they are expected to be applied in a variety of fields. The following sections describe the synthetic strategies, properties, and potential applications of OCFs.

3.2 Mechanism of formation

OCFs were prepared by a simple pyrolysis of a guest-free porphyrin molecular crystal with polymerizable moieties (**1-4**) in an inert gas atmosphere without any additional operations such as activation or acid wash.[33-36] During the heat treatment, the polymerizable moieties are crosslinked to form a crystalline polymer that is successively transformed into a carbonaceous framework with an ordered structure. Crystallographic structural changes upon carbonization process are summarized below using Ni$_2$-CPD$_{py}$ (**1**) as an example (Fig. 6). **1** possesses a slipped conformation with a distance of 9.7 Å between the two molecules (Fig. 6d). The diacetylene bridges are located in close proximity to those of the neighbouring molecules. The **1** molecules align along the c-axis to form columnar structure (Fig. 6e), and the columns assemble to form a crystal (Fig. 6f). When the crystal is heat-treated at 593 K, the diacetylene moieties next to each other are crosslinked to form polydiacetylene backbones (Fig. 6g), resulting in the formation of a two-dimensional sheet (Fig. 6h) which are stacked to form the polymer crystal (Fig. 6i). In other words, the

precursor molecular crystals are topochemically polymerized to form a kind of crystalline COF. Even after the subsequent carbonization at 873K, the structural regularity of the (020) plane of the polymer is well retained (Fig. 6j). This is confirmed by the PXRD pattern, which shows a sharp peak at almost the same *d*-spacing (14.8 Å) with that of the precursor polymer (14.6 Å) (Fig. 7a). The high angle annular dark-field scanning transmission electron microscopy (HAADF-STEM) image also visualized the regular arrangement of single-atomic Ni species (Fig. 7b), and the periodicity is in good agreement with the *d*-spacing determined by the PXRD pattern. Fig. 7b suggests that Ni species maintain their atomic-level dispersion in the carbon frameworks even after the heat treatment, which is also supported by the absence of diffraction derived from Ni metal or NiO in the PXRD pattern. These crystallographic studies clearly showed that the molecular crystals can be transformed into OCFs via the thermal solid-phase polymerization, which plays a pivotal role to retain the original periodic structure with reinforcing the frameworks. In the cases of the Ni and Fe porphyrin monomers (**2-4**), the acetylene moieties are in close each other in their crystals instead of the diacetylene in **1**. Thus, the acetylene moieties lead to topochemical polymerization and the eventual formation of OCFs.
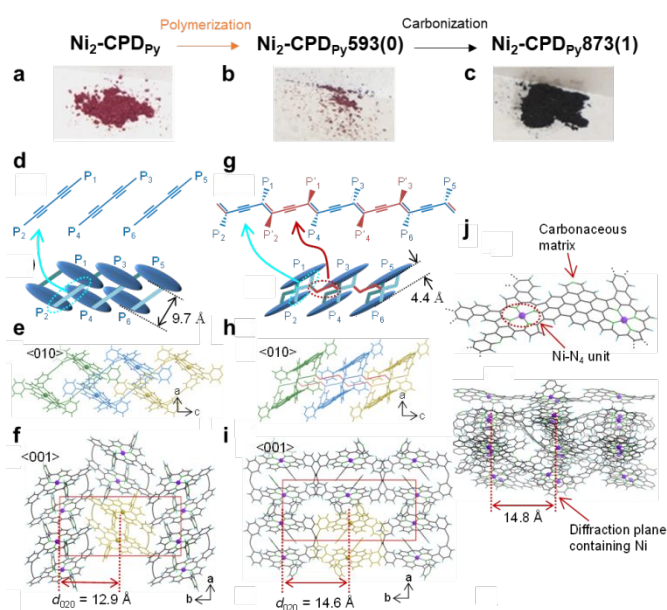

Fig. 6 Structural transformation from Ni_2-CPD_{Py} to OCFs. (a-c) Photographs of Ni_2-CPD_{Py} and heat-treated samples of Ni_2-CPD_{Py}X(Y): X and Y indicate heat treatment temperature (K) and holding time (h), respectively. Structures of (d, e, f) Ni_2-CPD_{Py}, (g, h, i) Ni_2-CPD_{Py}593(0), and (j) Ni_2-CPD_{Py}873(1).[33]
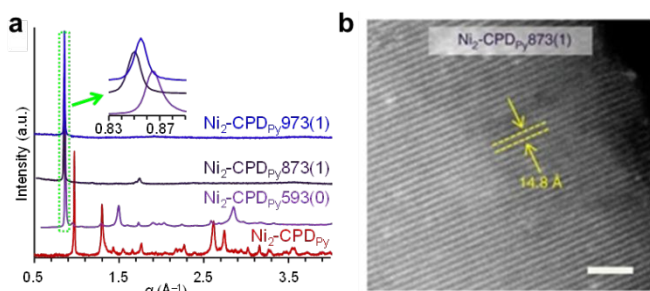
Fig. 7 (a) PXRD patterns of Ni_2-CPD_{Py} and heat-treated samples. (b) HAADF-STEM image of Ni_2-CPD_{Py}873(1).[33]

3.3 Characteristics of OCFs – Comparison with organic-based frameworks and conventional carbon materials

The properties of OCFs are summarized in Fig. 2 in comparison with organic-based frameworks (MOFs) and conventional microporous carbon materials.[6, 33, 36, 114, 115] In the following subsections, the characteristics of OCFs are discussed in detail.

3.3.1 Graphene-based ordered frameworks

The critical difference between OCFs and conventional organic-based frameworks, such as MOFs and COFs, is that the framework is composed of graphene sheets rather than organic ligands. OCFs are not organic molecules but are classified as carbon materials. The progress of carbonization can be determined from Raman spectra; the OCFs exhibited only broad D- and G-bands, indicating that the polymer was transformed into the defective graphene sheets (Fig. 8).[116] It is noteworthy that no stacking of graphene sheets was confirmed by the absence of carbon 002 peak at $2\theta = 26°$, in the PXRD pattern.[33-36] Such graphene frameworks afford OCFs chemical and thermal stabilities as well as electrical conductivity that are difficult to be achieved in organic-based frameworks like MOFs. In fact, the insulator Ni_2-CPD_{Py} turned into a conductor by heat treatment at 873 K: the resistivity of the resulting carbon was 33.8 Ω cm at room temperature.[33] These unique properties of OCFs unlike conventional organic-based frameworks pave the way for their electrochemical applications. Furthermore, porous OCFs composed of non-stacked graphene exhibited unique elasticity (for details, see Section 4.2).
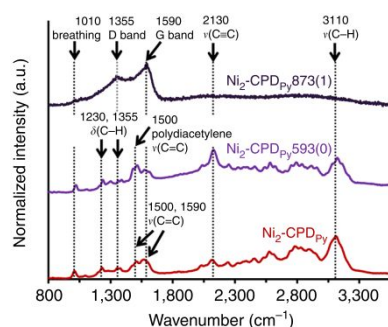

Fig. 8 Raman spectra of Ni_2-CPD_{Py} and heat-treated samples.[33]

3.3.2 Single-atomic metals in square planar coordination

The common feature of OCFs and MOFs is that they have periodic metal centres. In the case of MOFs, metal clusters (for example Zn_4O clusters in MOF-5) or metal ions (for example Zn ions in ZIF-8) are periodically arranged as building units.[67] OCFs also have a regular arrangement of single-atomic metal species in the ordered graphene frameworks. The metal (M) forms a planar four-coordinate structure (M-N_4 coordination units) derived from the precursor metalloporphyrins, which is different from the

tetrahedral coordination unit of ZIF-8.[67] The local structure of metals can be analysed by X-ray absorption fine structure (XAFS) measurements. Characteristic pre-edges are observed in the X-ray absorption near edge structure (XANES) spectra (8836 eV for Ni[33, 34, 36], 7113 eV for Fe[35]), which were evidence that the OCFs has planar four-coordination.[117, 118] The pseudo-radial structure functions, calculated from the extended X-ray absorption fine structure (EXAFS) spectra, displayed similar patterns to that of the precursor porphyrins for all reported OCFs, confirming the retention of the M–N_x coordination even after carbonization without aggregation to form nanoparticles.[33-36] Since M-N_x units are reported to catalyse many kinds of electrochemical reactions including ORR as mentioned in Section 2.2.2, OCFs are expected to be applied to such fields. When considering the practical application, the high metal content is a key feature of OCFs compared to conventional M-N-C catalysts; as an example, the OCF synthesized from **1** has a Ni content of more than 9 wt%.[33] It should be noted that the metal loadings in MOF-derived M-N-C catalysts are generally less than 1 wt%, and even the largest cases reported so far were around 4 wt%,[96-98, 119, 120] e.g., the Fe-N-C catalyst from PCN-22 (3.5 wt%)[119] and the Co-N-C catalyst from the bimetallic Zn/Co ZIF (4.3 wt%).[96]

3.3.3 Porous structures and their development process

Towards various applications of OCFs, e.g., supercapacitors, gas separation, gas storage, and catalysis, high specific surface area as well as developed porosity is demanded. However, the first OCF synthesized from **1** had a low specific surface area of 43 m^2 g^{-1}.[33] By contrast, MOFs generally exhibit a specific surface area of several thousand m^2 g^{-1}. For example, MOF-177 recorded 4500 m^2 g^{-1}.[115] Very recently, the authors have found that the increase of polymerizable ethynyl groups is effective to increase the specific surface area of OCFs.[36] As shown in N_2 adsorption/desorption isotherms in Fig. 9a, the precursor molecule of **4** is poorly porous (11 m^2 g^{-1}) and no significant enhancement was observed even after the thermal polymerization at 553 K (**4_553(0)**; 55 m^2 g^{-1}). In contrast, the microporosity was significantly developed by the carbonization process at 873 K, and the largest recorded S_{BET} of 673 m^2 g^{-1} (**4_873(1)**) was achieved in OCFs reported thus far. The S_{BET} remarkably decreased with the collapse of the ordered structure by the heat treatment at 973 K (**4_973(0)**). Interestingly, the micropore sizes of the OCFs are uniform (Fig. 9b), suggesting that the micropores have been developed in the ordered frameworks. Similar micropore development during the carbonization was also observed in the OCF synthesis from the Ni porphyrin monomer with two ethynyl groups (**2**), but with a maximum specific surface area of 276 m^2 g^{-1}.[34] Therefore, the enhancement of micropores OCFs derived from **4** can be attributed to a large number of polymerizable ethynyl groups. Further development of nanopores, to be comparable to these of MOFs, will lead to wider application of OCFs.
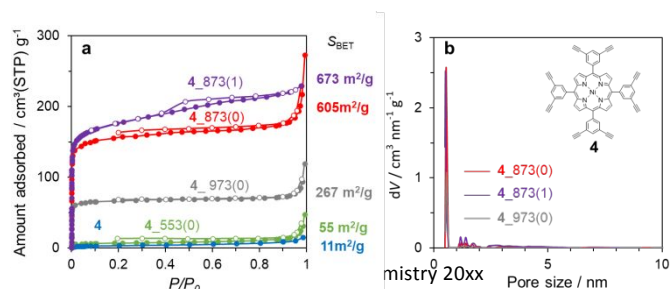
Fig. 9 (a) N_2 adsorption/desorption isotherms and (b) pore size distributions calculated by DFT method of **4** and the heat-treated samples of **4_X(Y)**: X and Y indicate heat treatment temperature (K) and holding time (h), respectively. Reprinted with permission.[36] Copyright 2021 Royal Society of Chemistry.

3.4 Requirements of OCF precursors

Organic molecules and polymers generally turn into disordered carbonaceous structures by heat treatment. The authors have found four types of exceptional precursors (**1-4**) that are converted into carbons with ordered structures.[33-36] Herein, we extract the crucial factors required in the exceptional precursors for obtaining OCFs (Fig. 10):

(i) A precursor molecule should contain thermally polymerizable moieties that eventually transform into carbon frameworks.

(ii) A precursor molecule should contain thermally stable blocks such as metalloporphyrin units up to carbonization temperature.

(iii) Precursor molecules should form a crystalline packing structure.

(iv) Upon thermal polymerization of a precursor, a crystalline polymer should be formed rather than an amorphous polymer.

The details of each requirement are explained below as a guideline towards the further expansion of the OCF family.
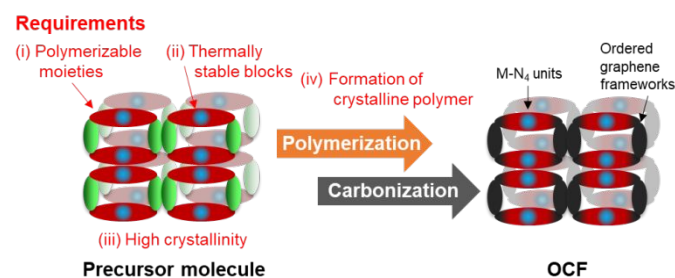

Fig. 10 Requirements for the OCF precursors.

3.4.1 Requirement (i): Thermally polymerizable moieties

The Ni cyclic porphyrin dimer (**1**), the first OCF precursor, contains diacetylene moieties which are polymerized during the heat treatment process and eventually turned into a carbon framework.[33] Also, acetylene moieties (ethynyl groups) in **2-4** function as polymerizable moieties.[34-36] Since the role of polymerization moieties has been already discussed, this section focus on how to determine the occurrence of thermal polymerization and its temperature. The direct method is thermogravimetry (TG) and differential scanning calorimetry (DSC) in an inert gas atmosphere. As shown in Fig. 11, a porphyrin monomer **5** without polymerizable moieties (Ni(II) tetraphenylporphyrin) has no DSC peak. In contrast, both Ni and H_2 porphyrins containing two ethynyl groups (**2, 6**) showed a distinct exothermic peak at around 580 K without significant weight loss in the TG profile. These features clearly indicate the thermal polymerization without thermal decomposition involving gas emission. The formation of crosslinking structures can be examined by some spectroscopy techniques. The progress of polymerization can be understood by observing the $\nu(C\equiv C)$ band at 2254 cm^{-1} in

Raman measurement.[33] Also, the disappearance of the peak due to sp bonds in ^{13}C NMR spectrum is the evidence of polymerization.[33, 34, 36]
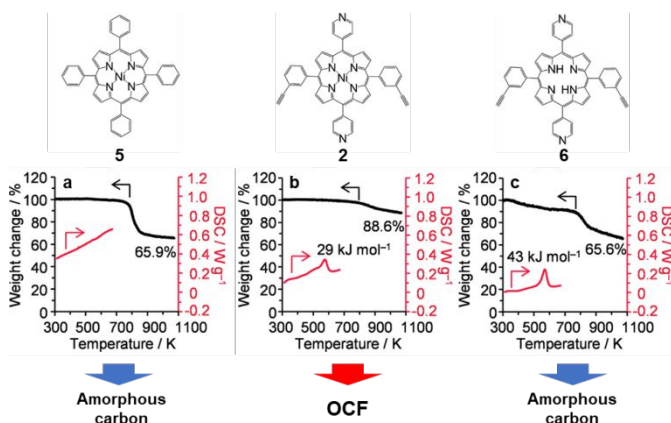

Fig. 11 TG-DSC profiles of three porphyrin monomers: (a) Ni(II) tetraphenylporphyrin and (b) Ni and (c) H_2 porphyrins containing two ethynyl groups. Reprinted with permission.[34] Copyright 2020 Chemical Society of Japan.

3.4.2 Requirement (ii): Thermally stable blocks

While both **2** and **6** have thermally polymerizable moieties (Fig. 11), only **2** forms OCF via the carbonization. This is because the lack of "thermally stable blocks" in **6**. In the TG profile (Fig. 11), the yield of **6** at 1073 K was 65.6%, significantly lower than those of **2** (88.6%). The deference can be attributed to the lower thermal stability of the H_2 porphyrin unit compared to the Ni one, causing the structural collapse at around 800 K. Indeed, it has been reported that H_2 porphyrin ring is decomposed to release pyrrole fragments during the pyrolysis around 573-873 K.[33] Thus, the precursors for OCFs found so far all contain metalloporphyrin units as thermally stable blocks.[33-36] The thermal stability of functional groups around the metalloporphyrin ring also greatly affect the OCF formation. The Ni-porphyrin monomer with pyridyl groups (**2**) retained its ordered structure, while the one with mesityl groups yielded an amorphous structure.[34, 36] Mass spectroscopy during thermogravimetry-differential measurements (TG-DSC-MS) revealed that the mesityl groups desorbed at around 800 K, which led to a decrease in the carbonization yield (around 70%). TG results can be used as an indicator to determine if a molecule has the potential to be an OCF precursor: no significant weight loss at around 800 K and high carbonization yield (typically >85%).

3.4.3 Requirement (iii): High crystallinity of precursors

Non-crystalline molecules have never yielded OCFs, even if requirements (i) and (ii) are satisfied. Molecules with the same porphyrin unit may have different packing structures depending on the metal centre; the cyclic porphyrin dimer is a good example.[33] In contrast to the Ni case (**1**), the cyclic Fe porphyrin dimer has no crystalline structure, and thus, a carbon with amorphous structure is produced. In addition, obtaining highly crystalline precursor molecules through recrystallization process is an important step for reproducible preparation of OCFs. The crystallinity of the precursor

greatly affects the degree of regularity of the resulting carbonaceous framework and the suppression of metal aggregation in our experience.

3.4.4 Requirements (iv): Formation of a crystalline polymer

In addition to the above requirements (i)-(iii), the formation of a crystalline polymer upon thermal polymerization is an essential factor for the OCF synthesis. For example, tetraphenylmethane with four ethynyl groups is a crystalline molecule with polymerizable moieties and a thermally stable tetraphenylmethane block. Upon heating, the molecules are turned into a polymer at 503 K and further carbonized with a high yield of 89%. However, the polymer is amorphous, and therefore, a disordered carbon material is formed.[121] In some cases, a slight difference in the molecular structure has a profound impact on the final carbon structure. The Fe porphyrin with two ethynyl groups at *meta*-position (**3**) yielded OCFs, whereas in the case of *para*-position, the ordered structure collapsed upon polymerization, yielding a disordered carbon material.[35] By contrast, in the successful OCF synthesis from **1**-**4**, crystalline polymers are always formed around 573–723 K. A key factor to form crystalline polymers may be the distance between the polymerizable moieties. In the field of photopolymerization, the distance between the polymerizable moieties in monomer molecules has been found to be a crucial factor for structure-preserving solid-state polymerization, or topochemical polymerization.[122] The appropriate stacking distance of diacetylene monomers is 5 Å, so called the "5 Å rule",[122-125] which provides insight into the OCF synthesis via thermal polymerization. In fact, in the OCF precursor crystals discovered so far, the diacetylene or acetylene moieties are close together less than 5 Å (closest distance **1**: 4.3 Å, **2**: 4.8 Å, **3**: 3.7 Å, **4**: 3.5 Å).[33-36] The synthesis of precursor molecular crystals in which the polymerizable moieties are sufficiently close to each other would be a promising strategy for exploring OCF precursors. Nevertheless, these tactics is not perfect, and it is actually difficult to completely predict which molecules will turn into crystalline polymers or not at the present state-of-art though.

4. Unique functions of OCFs

4.1 Electrocatalysis

One of the interesting features of OCFs is high density M-N_4 sites embedded in highly conductive frameworks, which are favourable to promote various electrocatalytic reactions.[82-87] Since MOFs and COFs are not conductive, they need to be combined with conductors for electrochemical applications.[79-81] In contrast, OCFs intrinsically possess electrical conductivity owing to the graphene-based frameworks, and OCFs themselves function as conductive matrix. Fig. 12 shows the electrochemical CO_2 reduction activity over the OCF synthesized from **1** (Ni$_2$-CPD$_{Py}$973(1)) along with three reference catalysts.[33] The OCF exhibited obvious catalytic activity for the CO_2 conversion to CO even without conductive additives, while the activity for H_2 generation was quite low. Thus, high Faraday efficiencies of 94% and 87% were achieved

at −0.8 V and −0.9 V, respectively. ZTC, an ordered microporous carbon without metals, was inactive for the CO_2 conversion, indicating that Ni species acted as catalytic active sites. Furthermore, both the Ni_2-CPD_{Py} precursor (**1**) and Ni-TPP973(1), the carbon with Ni aggregates synthesized by the carbonization of Ni-tetraphenylporphyrin (**5**), gave no catalytic performance. Thus, the combination of Ni-N_4 coordination units and electrically conductive graphene-based framework rendered OCFs unique efficient catalysts for CO_2 conversion. Such a high performance has also been obtained by OCFs synthesized from porphyrin monomers. The Ni-containing OCF from **2** achieved 92% Faraday efficiency for CO at -0.8V,[34] and the Fe-containing OCF from **3** also catalysed the reaction with significantly higher efficiency than the catalyst without the Fe–N_4 coordination units.[35]

OCFs have a great potential for a wide variety of electrocatalysis applications including ORR from their structure designability of OCFs in which the immobilization of various metal species on graphene frameworks is possible.
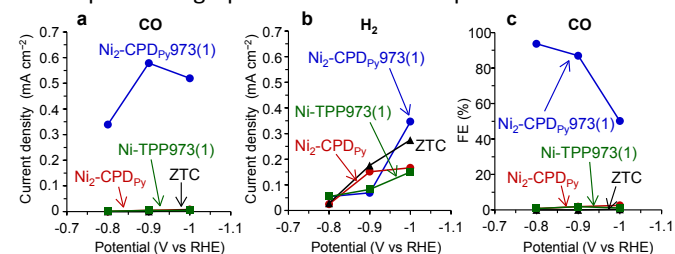

Fig. 12 Partial current densities used for (a) CO and (b) H_2 generation, and (c) Faraday efficiency for CO generation in electrocatalytic CO_2 conversion over the OCF from Ni_2-CPD_{Py} (**1**) and reference samples.[33]

4.2 Force-responsive property

As shown in Section 3.2.3, OCFs with well-developed micropores can be synthesized by increasing the number of crosslinking moieties.[36] Such porous OCFs can be considered as a kind of graphene-based nanoporous materials which are analogies of ZTC and graphene mesosponge (GMS).[13, 21, 22, 24, 126] The authors have previously revealed that single-graphene frameworks of ZTC and GMS make them extraordinarily flexible despite their small pore size (<10 nm). Such nanoporous flexible materials function as an elastic nanosponge, leading to a new phenomenon of force-responsive phase transitions.[22] Based on these studies, the mechanical flexibility of porous OCFs has been investigated by *in-situ* methanol-vapour adsorption/desorption measurement with and without the stress application.[36] As shown in Fig. 13a, when the porous OCF was pressed at a pressure of 213 MPa, there was a clear decrease in the amount of methanol adsorbed. When the force is released and measured again, the adsorption amount is almost the same as that before pressurization. These results indicate that the micropores in OCFs are contracted by mechanical force and recovered to their original state upon release. The force-induced liquid-gas phase transition was further demonstrated in Fig. 13b. The methanol vapor pressure inside a sample chamber repeatedly

rises and falls in response to the application and release of stress. Thus, the porous OCF functioned as an elastic nanosponge; adsorbates in the porous OCF are desorbed (evaporation) by force application and re-adsorbed (condensation) by release (Fig. 13c). The combination with regularly aligned single-atomic catalytically active sites will open up new applications for force-responsive electrocatalysts, just like cytochrome complexes.[127]
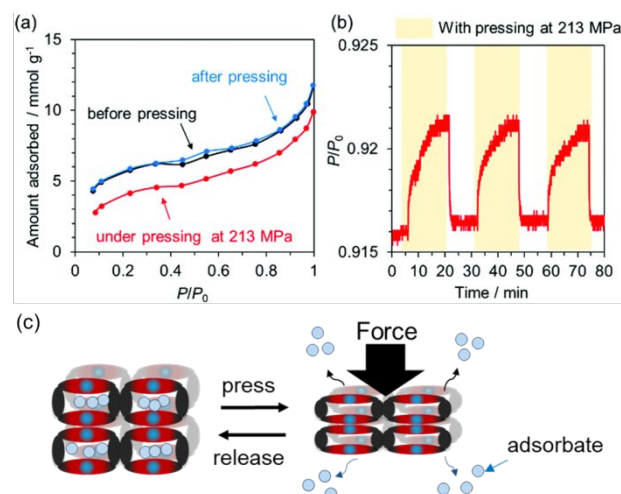

Fig. 13 (a) Methanol adsorption isotherms (298 K) of the OCF from **4** before (black), under (red) and after (blue) the application of a mechanical force (213 MPa). (b) Fluctuation of methanol vapour pressure inside the chamber during applying/releasing a mechanical force to the OCF from **4**. (c) Schematic illustration of force-driven phase transition. Reprinted with permission.[36] Copyright 2021 Royal Society of Chemistry.

5. Conclusions and perspective

The development and applications of OCFs have been summarized in this feature article. Since the discovery of the structure-preserving carbonization of Ni cyclic porphyrin dimers in 2017, four OCF precursors have been found thus far. By summarizing these studies, the authors have discussed the mechanism for OCF formation and the requirements of OCF precursor molecules. Polymerizable moieties in a precursor crosslink each other to form a crystalline polymer, which is eventually transformed into the ordered graphene frameworks. At the same time, the thermally stable metalloporphyrin blocks retains M-N_4 coordination units even after the carbonization, and the M-N_4 units are incorporated into the conductive graphene frameworks of OCFs. The structures of OCFs can be determined more precisely at a molecular level than that of conventional disordered microporous carbons, which is a great advantage in understanding the relationship between the chemical structure of carbons and their properties as well as performance. The unique features of OCFs, such as conductive graphene frameworks, regularly aligned single-metal species, and developed microporosity, make them promise for a wide variety of applications. OCFs

ARTICLE

have already shown high performance in electrocatalytic CO_2 reduction and unique force-responsible properties, paving the way for further applications.

Although there have been still limited examples of OCF synthesis thus far, the design and synthesis of precursors will expand the OCF family to a wide variety of chemical and pore structures, like MOFs. The precursor requirements presented in this paper will help the further development of new types of OCFs. All the precursors of OCFs synthesized so far contain metalloporphyrin blocks, but the thermally stable blocks are not limited to porphyrin units. There are many candidates for further expansion of the OCF family, including phthalocyanine and polycyclic aromatics. There is also plenty of room to design the type and number of polymerizable moieties. As mentioned above, the maximum specific surface area of the OCFs synthesized so far is 673 m^2/g, which is not as high as that of conventional microporous carbons and MOFs. Further development of specific surface area is desirable towards wider application of OCFs. Recently, carbon materials with controlled pore size at an angstrom level have been fabricated by carbonizing tetraphenylmethane and tetrabiphenylmethane, three-dimensional aromatic molecules with ethynyl groups.[121] The four ethynyl groups induce isotropic and rigid 3D cross-linking upon heat treatment, thus the pore size of resulting carbons can be controlled by the length of the phenyl or biphenyl moieties. Thus, it is expected that future development of molecular design will enable flexible and precise control of framework structures in the OCF family.

Additionally, extending the range of metal types to Co, Cu, Zn, Ru, and Pt will further expand the potential of applications, especially for catalytic applications. In the case of COFs, various electrochemical catalytic reactions are promoted depending on types of immobilized single-atomic metal species. For example, Pt promotes hydrogen evolution and hydrogen oxidation reactions, while Cu and Ni catalyse nitrogen oxide and CO_2 reduction, respectively.[81] In addition, single atomic catalysts with Pt, Pd, and Au have been reported to significantly outperform conventional nanoparticle catalysts in various selective organic synthesis reactions, including semi-hydrogenation and hydrochlorination.[128-130] The development of catalytic functions is expected through the expansion of metal species while taking advantage of the high metal loading and thermal stability of OCFs.

Scalable synthesis is an important factor in the future development of such applications. The valuable advantages of OCF production are a simple procedure of "just annealing" and a high carbonization yield (>80 %). Thus, the scalability depends on the producibility of the precursor. At the first reported OCFs, the precursor (Ni cyclic porphyrin dimer) was synthesized in multiple steps and only the production of several tens mg was possible.[33, 113] Later on, the precursors of OCFs were expanded to metalloporphyrin monomers which can be synthesized by gram scale. The exploration of more scalable and inexpensive precursors will further enhance the feasibility of OCFs for practical applications.

The authors hope that this feature article will provide a guideline for further synthesis of carbons with molecular-level design and contribute to understanding and development of carbon materials science.

Conflicts of interest

There are no conflicts to declare.

Acknowledgements

References

1. I. C. Gerber and P. Serp, *Chem. Rev.*, 2020, **120**, 1250-1349.
2. S. Fa, M. Yamamoto, H. Nishihara, H. Nishihara, R. Sakamoto, K. Kamiya, K. Kamiya, Y. Nishina, T. Ogoshi and T. Ogoshi, *Chem. Sci.*, 2020, **11**, 5866-5873.
3. Y. Kawabuchi, H. Oka, S. Kawano, I. Mochida and N. Yoshizawa, *Carbon*, 1998, **36**, 377-382.
4. E. Kayahara, T. Iwamoto, H. Takaya, T. Suzuki, M. Fujitsuka, T. Majima, N. Yasuda, N. Matsuyama, S. Seki and S. Yamago, *Nat. Commun.*, 2013, **4**, 2694.
5. N. Rangnekar, N. Mittal, B. Elyassi, J. Caro and M. Tsapatsis, *Chem. Soc. Rev.*, 2015, **44**, 7128-7154.
6. S. Kitagawa, R. Kitaura and S.-I. Noro, *Angew. Chem. Int. Ed.*, 2004, **43**, 2334-2375.
7. T. Kyotani, *Bull. Chem. Soc. Jpn.*, 2006, **79**, 1322-1337.
8. M. T. Gilbert, J. H. Knox and B. Kaur, *Chromatographia*, 1982, **16**, 138-146.
9. T. Kyotani, T. Nagai, S. Inoue and A. Tomita, *Chem. Mater.*, 1997, **9**, 609-615.
10. Z. Ma, T. Kyotani and A. Tomita, *Chem. Commun.* , 2000, 2365-2366.
11. Z. Ma, T. Kyotani, Z. Liu, O. Terasaki and A. Tomita, *Chem. Mater.*, 2001, **13**, 4413-4415.
12. H. Nishihara, Q.-H. Yang, P.-X. Hou, M. Unno, S. Yamauchi, R. Saito, J. I. Paredes, A. Martínez-Alonso, J. M. D. Tascón, Y. Sato, M. Terauchi and T. Kyotani, *Carbon*, 2009, **47**, 1220-1230.
13. H. Nishihara and T. Kyotani, *Chem. Commun.*, 2018, **54**, 5648-5673.
14. H. Nishihara, K. Imai, H. Itoi, K. Nomura, K. Takai and T. Kyotani, *Tanso*, 2017, **2017**, 169-174.
15. H. Nishihara, H. Fujimoto, H. Itoi, K. Nomura, H. Tanaka, M. T. Miyahara, P. A. Bonnaud, R. Miura, A. Suzuki, N. Miyamoto, N. Hatakeyama, A. Miyamoto, K. Ikeda, T. Otomo and T. Kyotani, *Carbon*, 2018, **129**, 854-862.

16. R. Ryoo, S. H. Joo and S. Jun, *J. Phys. Chem. B*, 1999, **103**, 7743-7746.
17. J. Lee, S. Yoon, T. Hyeon, S. M. Oh and K. B. Kim, *Chem. Commun.* , 1999, 2177-2178.
18. A. A. Zakhidov, R. H. Baughman, Z. Iqbal, C. Cui, I. I. Khayrullin, S. O. Dantas, J. Marti and V. G. Ralchenko, *Science*, 1998, **282**, 897-901.
19. F. Wang, T. Hou, X. Zhao, W. Yao, R. Fang, K. Shen and Y. Li, *Adv. Mater.*, 2021, **33**, e2102690.
20. Z. Chen, W. Ren, L. Gao, B. Liu, S. Pei and H. M. Cheng, *Nat. Mater.*, 2011, **10**, 424-428.
21. H. Nishihara, T. Simura, S. Kobayashi, K. Nomura, R. Berenguer, M. Ito, M. Uchimura, H. Iden, K. Arihara, A. Ohma, Y. Hayasaka and T. Kyotani, *Adv. Funct. Mater.*, 2016, **26**, 6418-6427.
22. K. Nomura, H. Nishihara, M. Yamamoto, A. Gabe, M. Ito, M. Uchimura, Y. Nishina, H. Tanaka, M. T. Miyahara and T. Kyotani, *Nat. Commun.*, 2019, **10**, 2559.
23. K. Nomura, H. Nishihara, N. Kobayashi, T. Asada and T. Kyotani, *Energy Environ. Sci.*, 2019, **12**, 1542-1549.
24. S. Sunahiro, K. Nomura, S. Goto, K. Kanamaru, R. Tang, M. Yamamoto, T. Yoshii, J. N. Kondo, Q. Zhao, A. G. Nabi, R. Crespo-Otero, D. Di Tommaso, T. Kyotani and H. Nishihara, *J. Mater. Chem. A*, 2021, **9**, 14296-14308.
25. C. Liang, K. Hong, G. A. Guiochon, J. W. Mays and S. Dai, *Angew. Chem. Int. Ed.*, 2004, **43**, 5785-5789.
26. S. Tanaka, N. Nishiyama, Y. Egashira and K. Ueyama, *Chem. Commun.*, 2005, 2125-2127.
27. Y. Meng, D. Gu, F. Zhang, Y. Shi, H. Yang, Z. Li, C. Yu, B. Tu and D. Zhao, *Angew. Chem. Int. Ed.*, 2005, **44**, 7053-7059.
28. H. Nishihara and T. Kyotani, *Adv. Mater.*, 2012, **24**, 4473-4498.
29. B. Liu, H. Shioyama, T. Akita and Q. Xu, *J. Am. Chem. Soc.*, 2008, **130**, 5390-5391.
30. M. Hu, J. Reboul, S. Furukawa, N. L. Torad, Q. Ji, P. Srinivasu, K. Ariga, S. Kitagawa and Y. Yamauchi, *J. Am. Chem. Soc.*, 2012, **134**, 2864-2867.
31. J.-K. Sun and Q. Xu, *Energy Environ. Sci.*, 2014, **7**, 2071-2100.
32. W. Chaikittisilp, K. Ariga and Y. Yamauchi, *J. Mater. Chem. A*, 2013, **1**, 14-19.
33. H. Nishihara, T. Hirota, K. Matsuura, M. Ohwada, N. Hoshino, T. Akutagawa, T. Higuchi, H. Jinnai, H. Koseki, H. Kasai, Y. Matsuo, J. Maruyama, Y. Hayasaka, Y. Yamada, S. Yamaguchi, K. Kamiya, T. Kamimura, H. Nobukuni and F. Tani, *Nat. Commun.*, 2017, **8**, 109.
34. H. Nishihara, K. Matsuura, M. Ohwada, M. Yamamoto, Y. Matsuo, J. Maruyama, Y. Hayasaka, S. Yamaguchi, K. Kamiya, H. Konaka, M. Inoue and F. Tani, *Chem. Lett.*, 2020, **49**, 619-623.
35. M. Yamamoto, K. Takahashi, M. Ohwada, Y. Wu, K. Iwase, Y. Hayasaka, H. Konaka, H. Cove, D. Di Tommaso, K. Kamiya, J. Maruyama, F. Tani and H. Nishihara, *Catal. Today*, 2021, **364**, 164-171.
36. K. Chida, T. Yoshii, K. Takahashi, M. Yamamoto, K. Kanamaru, M. Ohwada, V. Deerattrakul, J. Maruyama, K. Kamiya, Y. Hayasaka, M. Inoue, F. Tani and H. Nishihara, *Chem. Commun.* , 2021, **57**, 6007-6010.
37. H. L. Jiang, B. Liu, Y. Q. Lan, K. Kuratani, T. Akita, H. Shioyama, F. Zong and Q. Xu, *J. Am. Chem. Soc.*, 2011, **133**, 11854-11857.

38. L. Radhakrishnan, J. Reboul, S. Furukawa, P. Srinivasu, S. Kitagawa and Y. Yamauchi, *Chem. Mater.*, 2011, **23**, 1225-1231.
39. B. Liu, H. Shioyama, H. Jiang, X. Zhang and Q. Xu, *Carbon*, 2010, **48**, 456-463.
40. D. Yuan, J. Chen, S. Tan, N. Xia and Y. Liu, *Electrochem. Commun.*, 2009, **11**, 1191-1194.
41. T. Kitao, M. W. A. MacLean, K. Nakata, M. Takayanagi, M. Nagaoka and T. Uemura, *J. Am. Chem. Soc.*, 2020, **142**, 5509-5514.
42. J. Hu, H. Wang, Q. Gao and H. Guo, *Carbon*, 2010, **48**, 3599-3606.
43. M. Hu, J. Reboul, S. Furukawa, L. Radhakrishnan, Y. Zhang, P. Srinivasu, H. Iwai, H. Wang, Y. Nemoto, N. Suzuki, S. Kitagawa and Y. Yamauchi, *Chem. Commun.* , 2011, **47**, 8124-8126.
44. W. Chaikittisilp, M. Hu, H. Wang, H. S. Huang, T. Fujita, K. C. Wu, L. C. Chen, Y. Yamauchi and K. Ariga, *Chem. Commun.* , 2012, **48**, 7259-7261.
45. N. L. Torad, M. Hu, Y. Kamachi, K. Takai, M. Imura, M. Naito and Y. Yamauchi, *Chem. Commun.* , 2013, **49**, 2521-2523.
46. S. J. Yang, T. Kim, J. H. Im, Y. S. Kim, K. Lee, H. Jung and C. R. Park, *Chem. Mater.*, 2012, **24**, 464-470.
47. S. J. Yang, S. Nam, T. Kim, J. H. Im, H. Jung, J. H. Kang, S. Wi, B. Park and C. R. Park, *J. Am. Chem. Soc.*, 2013, **135**, 7394-7397.
48. H. B. Aiyappa, P. Pachfule, R. Banerjee and S. Kurungot, *Cryst. Growth Des.*, 2013, **13**, 4195-4199.
49. S. Lim, K. Suh, Y. Kim, M. Yoon, H. Park, D. N. Dybtsev and K. Kim, *Chem. Commun.* , 2012, **48**, 7447-7449.
50. K. Nakatsuka, T. Yoshii, Y. Kuwahara, K. Mori and H. Yamashita, *Chem. Eur. J*, 2018, **24**, 898-905.
51. B. You, N. Jiang, M. Sheng, W. S. Drisdell, J. Yano and Y. Sun, *ACS Catal.*, 2015, **5**, 7068-7076.
52. Z. Wang, T. Yan, J. Fang, L. Shi and D. Zhang, *J. Mater. Chem. A*, 2016, **4**, 10858-10868.
53. T. Jiang, W. Jiang, Y. Li, Y. Xu, M. Zhao, M. Deng and Y. Wang, *Carbon*, 2021, **180**, 92-100.
54. A. A. Dubale, I. N. Ahmed, X.-H. Chen, C. Ding, G.-H. Hou, R.-F. Guan, X. Meng, X.-L. Yang and M.-H. Xie, *J. Mater. Chem. A*, 2019, **7**, 6062-6079.
55. J. S. Li, S. L. Li, Y. J. Tang, K. Li, L. Zhou, N. Kong, Y. Q. Lan, J. C. Bao and Z. H. Dai, *Sci. Rep.*, 2014, **4**, 5130.
56. Q. Ren, H. Wang, X. F. Lu, Y. X. Tong and G. R. Li, *Adv. Sci.*, 2018, **5**, 1700515.
57. C. Wang, J. Kim, J. Tang, M. Kim, H. Lim, V. Malgras, J. You, Q. Xu, J. Li and Y. Yamauchi, *Chem*, 2020, **6**, 19-40.
58. X. Hu, X. Liu, K. Chen, G. Wang and H. Wang, *J. Mater. Chem. A*, 2019, **7**, 11016-11037.
59. J.-P. Song, L. Wu, W.-D. Dong, C.-F. Li, L.-H. Chen, X. Dai, C. Li, H. Chen, W. Zou, W.-B. Yu, Z.-Y. Hu, J. Liu, H.-E. Wang, Y. Li and B.-L. Su, *Nanoscale*, 2019, **11**, 6970-6981.
60. J. Tang, R. R. Salunkhe, J. Liu, N. L. Torad, M. Imura, S. Furukawa and Y. Yamauchi, *J. Am. Chem. Soc.*, 2015, **137**, 1572-1580.
61. L.-F. Chen, Y. Lu, L. Yu and X. W. Lou, *Energy Environ. Sci.*, 2017, **10**, 1777-1783.
62. C. Wang, C. Liu, J. Li, X. Sun, J. Shen, W. Han and L. Wang, *Chem. Commun.* , 2017, **53**, 1751-1754.
63. X. Chu, F. Meng, T. Deng and W. Zhang, *Nanoscale*, 2021, **13**, 5570-5593.

64. A. Mohanty, D. Jaihindh, Y.-P. Fu, S. P. Senanayak, L. S. Mende and A. Ramadoss, *J. Power Sources*, 2021, **488**, 229444.
65. J. Ren, Y. Huang, H. Zhu, B. Zhang, H. Zhu, S. Shen, G. Tan, F. Wu, H. He, S. Lan, X. Xia and Q. Liu, *Carbon Energy*, 2020, **2**, 176-202.
66. Y. Zheng, S. Zheng, H. Xue and H. Pang, *J. Mater. Chem. A*, 2019, **7**, 3469-3491.
67. H. B. Wu and X. W. Lou, *Sci. Adv.*, 2017, **3**, eaap9252.
68. L. Du, L. Xing, G. Zhang and S. Sun, *Carbon*, 2020, **156**, 77-92.
69. Q. Wang and D. Astruc, *Chem. Rev.*, 2020, **120**, 1438-1511.
70. A. Han, B. Wang, A. Kumar, Y. Qin, J. Jin, X. Wang, C. Yang, B. Dong, Y. Jia, J. Liu and X. Sun, *Small Methods*, 2019, **3**, 1800471.
71. N. Cheng, L. Ren, X. Xu, Y. Du and S. X. Dou, *Adv. Energy Mater.*, 2018, **8**, 1801257.
72. P. Pachfule, D. Shinde, M. Majumder and Q. Xu, *Nat. Chem.*, 2016, **8**, 718-724.
73. L. K. Shrestha, R. G. Shrestha, Y. Yamauchi, J. P. Hill, T. Nishimura, K. Miyazawa, T. Kawai, S. Okada, K. Wakabayashi and K. Ariga, *Angew. Chem. Int. Ed.*, 2015, **54**, 951-955.
74. T. Ogoshi, K. Yoshikoshi, R. Sueto, H. Nishihara and T. A. Yamagishi, *Angew. Chem. Int. Ed.*, 2015, **54**, 6466-6469.
75. G. L. Chai, Z. Hou, D. J. Shu, T. Ikeda and K. Terakura, *J. Am. Chem. Soc.*, 2014, **136**, 13629-13640.
76. T. Yoshii, K. Nakatsuka, T. Mizobuchi, Y. Kuwahara, H. Itoi, K. Mori, T. Kyotani and H. Yamashita, *Org. Process Res. Dev.*, 2018, **22**, 1580-1585.
77. T. Yoshii, D. Umemoto, M. Yamamoto, Y. Kuwahara, H. Nishihara, K. Mori, T. Kyotani and H. Yamashita, *ChemCatChem*, 2020, **12**, 5880-5887.
78. T. Yoshii, D. Umemoto, Y. Kuwahara, K. Mori and H. Yamashita, *ACS Appl. Mater. Interfaces*, 2019, **11**, 37708-37719.
79. P. Su, K. Iwase, T. Harada, K. Kamiya and S. Nakanishi, *Chem. Sci.*, 2018, **9**, 3941-3947.
80. Y. Wu, K. Kamiya, T. Hashimoto, R. Sugimoto, T. Harada, K. Fujii and S. Nakanishi, *Electrochemistry*, 2020, **88**, 359-364.
81. K. Kamiya, *Chem. Sci.*, 2020, **11**, 8339-8349.
82. G. Wu, K. L. More, C. M. Johnston and P. Zelenay, *Science*, 2011, **332**, 443-447.
83. M. Lefevre, E. Proietti, F. Jaouen and J. P. Dodelet, *Science*, 2009, **324**, 71-74.
84. W. J. Jiang, W. L. Hu, Q. H. Zhang, T. T. Zhao, H. Luo, X. Zhang, L. Gu, J. S. Hu and L. J. Wan, *Chem. Commun.*, 2018, **54**, 1307-1310.
85. T. Yoshii, K. Nakatsuka, Y. Kuwahara, K. Mori and H. Yamashita, *Chem. Lett.*, 2017, **46**, 789-791.
86. K. Nakatsuka, T. Yoshii, Y. Kuwahara, K. Mori and H. Yamashita, *Phys. Chem. Chem. Phys.*, 2017, **19**, 4967-4974.
87. T. Yoshii, K. Nakatsuka, Y. Kuwahara, K. Mori and H. Yamashita, *Rsc Adv*, 2017, **7**, 22294-22300.
88. M. Moriya, R. Takahama, K. Kamoi, J. Ohyama, S. Kawashima, R. Kojima, M. Okada, T. Hayakawa and Y. Nabae, *J. Phys. Chem. C*, 2020, **124**, 20730-20735.
89. T. Yoshii, K. Tamaki, Y. Kuwahara, K. Mori and H. Yamashita, *J. CO2 Util.*, 2021, **52**, 101691.
90. B. Chen, Z. Yang, Y. Zhu and Y. Xia, *J. Mater. Chem. A*, 2014, **2**, 16811-16831.
91. S. Ma, G. A. Goenaga, A. V. Call and D. J. Liu, *Chem. Eur. J*, 2011, **17**, 2063-2067.
92. D. Zhao, J.-L. Shui, C. Chen, X. Chen, B. M. Reprogle, D. Wang and D.-J. Liu, *Chem. Sci.*, 2012, **3**, 3200-3205.
93. X. X. Wang, D. A. Cullen, Y. T. Pan, S. Hwang, M. Wang, Z. Feng, J. Wang, M. H. Engelhard, H. Zhang, Y. He, Y. Shao, D. Su, K. L. More, J. S. Spendelow and G. Wu, *Adv. Mater.*, 2018, **30**, 1706758.
94. X. Pan, L. Bai, H. Wang, Q. Wu, H. Wang, S. Liu, B. Xu, X. Shi and H. Liu, *Adv. Mater.*, 2018, **30**, 1800180.
95. S. Wang, L. Shang, L. Li, Y. Yu, C. Chi, K. Wang, J. Zhang, R. Shi, H. Shen, G. I. Waterhouse, S. Liu, J. Tian, T. Zhang and H. Liu, *Adv. Mater.*, 2016, **28**, 8379-8387.
96. P. Yin, T. Yao, Y. Wu, L. Zheng, Y. Lin, W. Liu, H. Ju, J. Zhu, X. Hong, Z. Deng, G. Zhou, S. Wei and Y. Li, *Angew. Chem. Int. Ed.*, 2016, **55**, 10800-10805.
97. L. Jiao, J. Li, L. L. Richard, Q. Sun, T. Stracensky, E. Liu, M. T. Sougrati, Z. Zhao, F. Yang, S. Zhong, H. Xu, S. Mukerjee, Y. Huang, D. A. Cullen, J. H. Park, M. Ferrandon, D. J. Myers, F. Jaouen and Q. Jia, *Nat. Mater.*, 2021, **20**, 1385-1391.
98. L. Jiao, G. Wan, R. Zhang, H. Zhou, S. H. Yu and H. L. Jiang, *Angew. Chem. Int. Ed.*, 2018, **57**, 8525-8529.
99. Y. Chen, S. Ji, Y. Wang, J. Dong, W. Chen, Z. Li, R. Shen, L. Zheng, Z. Zhuang, D. Wang and Y. Li, *Angew. Chem. Int. Ed.*, 2017, **56**, 6937-6941.
100. R. Jiang, L. Li, T. Sheng, G. Hu, Y. Chen and L. Wang, *J. Am. Chem. Soc.*, 2018, **140**, 11594-11598.
101. X. Sun, A. I. Olivos-Suarez, D. Osadchii, M. J. V. Romero, F. Kapteijn and J. Gascon, *J. Catal.*, 2018, **357**, 20-28.
102. H. Zhang, S. Hwang, M. Wang, Z. Feng, S. Karakalos, L. Luo, Z. Qiao, X. Xie, C. Wang, D. Su, Y. Shao and G. Wu, *J. Am. Chem. Soc.*, 2017, **139**, 14143-14149.
103. Y. Meng, G. H. Wang, S. Bernt, N. Stock and A. H. Lu, *Chem. Commun.*, 2011, **47**, 10479-10481.
104. A. S. Hall, A. Kondo, K. Maeda and T. E. Mallouk, *J. Am. Chem. Soc.*, 2013, **135**, 16276-16279.
105. M. A. Reppy and B. A. Pindzola, *Chem. Commun.*, 2007, 4317-4338.
106. K. Hema, A. Ravi, C. Raju, J. R. Pathan, R. Rai and K. M. Sureshan, *Chem. Soc. Rev.*, 2021, **50**, 4062-4099.
107. R. H. Baughman, *J. Appl. Phys.*, 1972, **43**, 4362-4370.
108. S. Hayashi and K. Hayamizu, *Bull. Chem. Soc. Jpn.*, 1991, **64**, 685-687.
109. K. Hayamizu, S. Okada, S. Tsuzuki, H. Matsuda, A. Masaki and H. Nakanishi, *Bull. Chem. Soc. Jpn.*, 1994, **67**, 342-345.
110. H. Tanaka, M. A. Gomez, A. E. Tonelli and M. Thakur, *Macromolecules*, 1989, **22**, 1208-1215.
111. A. Sarkar, S. Okada, K. Komatsu, H. Nakanishi and H. Matsuda, *Macromolecules*, 1998, **31**, 5624-5630.
112. A. Sun, J. W. Lauher and N. S. Goroff, *Science*, 2006, **312**, 1030-1034.
113. H. Nobukuni, Y. Shimazaki, F. Tani and Y. Naruta, *Angew. Chem. Int. Ed.*, 2007, **46**, 8975-8978.
114. H. Itoi, H. Nishihara, T. Kogure and T. Kyotani, *J. Am. Chem. Soc.*, 2011, **133**, 1165-1167.
115. H. K. Chae, D. Y. Siberio-Pérez, J. Kim, Y. Go, M. Eddaoudi, A. J. Matzger, M. O'Keeffe and O. M. Yaghi, *Nature*, 2004, **427**, 523-527.

116.   M. J. Matthews, M. A. Pimenta, G. Dresselhaus, M. S. Dresselhaus and M. Endo, *Phys. Rev. B*, 1999, **59**, R6585-R6588.
117.   J. T. Miller, R. B. Fisher, A. M. J. Van Der Eerden and D. C. Koningsberger, *Energy Fuels*, 1999, **13**, 719-727.
118.   Q. Jia, N. Ramaswamy, H. Hafiz, U. Tylus, K. Strickland, G. Wu, B. Barbiellini, A. Bansil, E. F. Holby, P. Zelenay and S. Mukerjee, *ACS Nano*, 2015, **9**, 12496-12505.
119.   L. Jiao, R. Zhang, G. Wan, W. Yang, X. Wan, H. Zhou, J. Shui, S.-H. Yu and H.-L. Jiang, *Nat. Commun.*, 2020, **11**, 2831.
120.   Y. Pan, S. Liu, K. Sun, X. Chen, B. Wang, K. Wu, X. Cao, W. C. Cheong, R. Shen, A. Han, Z. Chen, L. Zheng, J. Luo, Y. Lin, Y. Liu, D. Wang, Q. Peng, Q. Zhang, C. Chen and Y. Li, *Angew. Chem. Int. Ed.*, 2018, **57**, 8614-8618.
121.   T. Ogoshi, Y. Sakatsume, K. Onishi, R. Tang, K. Takahashi, H. Nishihara, Y. Nishina, B. D. L. Campéon, T. Kakuta and T.-A. Yamagishi, *Commun. Chem.*, 2021, **4**, 75.
122.   A. Matsumoto, *Polym. J.*, 2003, **35**, 93-121.
123.   N. S. Goroff, S. M. Curtis, J. A. Webb, F. W. Fowler and J. W. Lauher, *Org. Lett.*, 2005, **7**, 1891-1893.
124.   S. M. Curtis, N. Le, F. W. Fowler and J. W. Lauher, *Cryst. Growth Des.*, 2005, **5**, 2313-2321.
125.   T. Odani, S. Okada, C. Kabuto, T. Kimura, H. Matsuda, A. Matsumoto and H. Nakanishi, *Chem. Lett.*, 2004, **33**, 1312-1313.
126.   M. Ito, H. Nishihara, K. Yamamoto, H. Itoi, H. Tanaka, A. Maki, M. T. Miyahara, S. J. Yang, C. R. Park and T. Kyotani, *Chem. Eur. J.*, 2013, **19**, 13009-13016.
127.   Z. Wang, T. Matsuo, S. Nagao and S. Hirota, *Org. Biomol. Chem.*, 2011, **9**, 4766-4769.
128.   N. Cheng, L. Zhang, K. Doyle-Davis and X. Sun, *Electrochem. Energy Rev.*, 2019, **2**, 539-573.
129.   G. Malta, S. A. Kondrat, S. J. Freakley, C. J. Davies, L. Lu, S. Dawson, A. Thetford, E. K. Gibson, D. J. Morgan, W. Jones, P. P. Wells, P. Johnston, C. R. Catlow, C. J. Kiely and G. J. Hutchings, *Science*, 2017, **355**, 1399-1403.
130.   G. Vile, D. Albani, M. Nachtegaal, Z. Chen, D. Dontsova, M. Antonietti, N. Lopez and J. Perez-Ramirez, *Angew. Chem. Int. Ed.*, 2015, **54**, 11265-11269.